Pairing of fermions in atomic traps and nuclei

H. Heiselberg
University of Southern Denmark, Campusvej 55, DK-5230 Odense M, Denmark
(Received 2 April 2003; published 24 November 2003)

Pairing gaps for fermionic atoms in harmonic-oscillator traps are calculated for a wide range of interaction strengths and particle numbers, and compared to pairing in nuclei. Especially systems where the pairing gap exceeds the single-level spacing but is smaller than the shell splitting $\hbar\omega$ are studied, which applies to most trapped Fermi atomic systems as well as to finite nuclei. When solving the gap equation for a large trap with such multilevel pairing, one finds that the matrix elements between nearby harmonic-oscillator levels and the quasi particle energies lead to a double logarithm of the gap, and a pronounced shell structure at magic numbers. It is argued that neutron and proton pairing in nuclei belongs to the class of multilevel pairing, that their shell structure follows naturally, and that the gaps scale as $\sim A^{-1/3}$—all in qualitative agreement with odd-even staggering of nuclear binding energies. Pairing in large systems is related to that in the bulk limit. For large nuclei the neutron and proton superfluid gaps approach the asymptotic value in infinite nuclear matter: $\Delta \simeq 1.1$ MeV.

DOI: 10.1103/PhysRevA.68.053616 PACS number(s): 03.75.Hh, 21.65.+f, 74.20.Fg, 67.60.−g

I. INTRODUCTION

Pairing in Fermi systems is central for understanding superconductivity in condensed-matter physics [1], superfluidity and glitches in neutron stars, excitation spectra and odd-even staggering of binding energies in nuclei [2], metallic clusters [3], and superconducting grains [4]. New insight into the general properties of such Fermi systems can now be obtained from experiments with atomic gases [5] which recently have been cooled down to degenerate temperatures around 10% of the Fermi temperature [6–9]. The interactions between trapped ^{6}Li and ^{40}K atoms have simultaneously been tuned above a Feshbach resonance, where they become strongly attractive, in order to produce optimal conditions for superfluidity [10]. Atomic gases have widely tunable number of particles, densities, interaction strengths, temperatures, spin states, and other parameters, which holds great promise for a more general understanding of pairing phenomena in solids, metallic clusters, grains, nuclei, and neutron stars.

In the experiments with ^{6}Li atoms the anisotropic expansion after sudden release from the trap is as predicted from hydrodynamics [11]. This is compatible both with a strongly interacting superfluid and collisional hydrodynamics. The scattering length is attractive $a<0$ and large such that densities above $\rho \gg 1/|a|^3$ are achieved and found mechanically stable against collapse. The interaction energy per particle, like Fermi energy, scales as $\rho^{2/3}$ [6–8] as predicted theoretically [12,13]. The superfluid gaps in bulk are also expected to be of the order of the Fermi energy.

In nuclear physics pairing is observed directly in the odd-even staggering of binding energies, i.e., nuclei with an even number of protons or neutrons are more strongly bound than nuclei with corresponding odd numbers by a pairing gap of the order of ~ 1 MeV. The same pairing gap also determines the excitation energies of ground-state nuclei. On average the pairing energies in nuclei decrease with the number of protons and neutrons modulated with a distinct shell structure, i.e., they are smaller near closed shells. It would be most interesting if the pairing gaps of fermionic atoms in harmonic-oscillator traps would display similar shell structure and scaling with the number of particles as nuclei.

The aim of this paper is to calculate pairing gaps in ultracold atomic Fermi gases in harmonic-oscillator traps and in nuclei, which are then compared to data on odd-even staggering of nuclear binding energies. For the atomic traps existing pairing gap calculations [14,15] are extended to systems, where level spectra and shell effects play an important role. It is shown that such pairing mechanisms are similar in nuclei, which to first approximation can be considered as a finite system of fermions in a harmonic-oscillator field with attractive δ-function interactions. Another important common feature is the anharmonic fields that lead to splitting of the single-particle states which reduce the pairing to the levels closest to the Fermi surface and leads to a distinct shell structure. For a wide range of interaction strengths and number of particles the trapped atomic clouds are predicted to display similar scaling and shell structure as nuclei as also seen in the experimental data on neutron and proton pairing. The scaling with particle number and the continuum or BCS limits are calculated for both large traps and nuclei and thereby the pairing gaps are estimated for nuclear matter, which also gives an idea about the superfluid gaps in neutron star matter.

The paper is organized as follows. In Sec. II the basic properties of interacting fermions in harmonic-oscillator traps are given, in particular the single-particle level spectra. Pairing is treated in Sec. III with individual sections devoted to each pairing regime where the last three sections outline the bulk, strongly interacting, and multilevel pairing regime. In Sec. IV we turn to nuclei and show that they belong to the class of multilevel pairing.

II. DILUTE FERMI GASES IN HARMONIC TRAPS

We treat a gas of N fermionic atoms of mass m in a harmonic-oscillator (HO) potential at zero temperature interacting via a two-body interaction with attractive s-wave scat-

tering length $a<0$. We shall mainly discuss a spherically symmetric trap and a dilute gas (i.e., where the density ρ obeys the condition $\rho|a|^3 \ll 1$) of particles with two spin states with equal population. The Hamiltonian is then given by

$$H=\sum_{i=1}^{N}\left(\frac{\mathbf{p}_i^2}{2m}+\frac{1}{2}m\omega^2\mathbf{r}_i^2\right)+g\sum_{i<j}\delta^3(\mathbf{r}_i-\mathbf{r}_j), \tag{1}$$

with the effective coupling $g=4\pi\hbar^2 a/m$. For a large number of particles N at zero temperature the Fermi energy is for a noninteracting system

$$E_F=(n_F+3/2)\hbar\omega\simeq(3N)^{1/3}\hbar\omega, \tag{2}$$

where $n_F\simeq(3N)^{1/3}$ is the HO quantum number at the Fermi surface. The HO shells are highly degenerate with states having angular momenta $l=n_F,n_F-2,\ldots,1$ or 0 due to the $U(3)$ symmetry of the three-dimensional spherically symmetric HO potential. However, interactions split this degeneracy. In the Thomas-Fermi (TF) approximation (see, e.g., Ref. [16]) the mean-field potential is

$$U(r)=\frac{1}{2}g\rho(r)=2\pi\frac{\hbar^2 a}{m}\rho(r), \tag{3}$$

the Fermi energy

$$E_F=\frac{\hbar^2 k_F^2(r)}{2m}+\frac{1}{2}m\omega^2 r^2+U(r). \tag{4}$$

The density can be determined from the Kohn-Sham energy density functionals. In a dilute gas the mean field is small as compared to the Fermi energy and its effect on the density can be ignored in the following. Thus

$$\rho(r)=k_F^3(r)/3\pi^2\simeq\rho_0(1-r^2/R_{TF}^2)^{3/2}, \tag{5}$$

inside the cloud $r\leqslant R_{TF}=a_{osc}\sqrt{2n_F+3}$, where $a_{osc}=\sqrt{\hbar/m\omega}$ is the oscillator length, and $\rho_0=(2n_F+3)^{3/2}/3\pi^2 a_{osc}^3$ is the central density [17].

The splitting of the HO shell degenerate levels $l=n_F,n_F-2,\ldots,1$ or 0 in the shell n_F by the mean-field potential can be calculated perturbatively in the dilute limit. An excellent approximation for the radial HO wave function with angular momentum l and $(n_F-l)/2$ radial nodes in the HO shell when $n_F\gg 1$ is the WKB one [18],

$$\mathcal{R}_{n_F l}(r)\simeq\frac{2}{\sqrt{\pi}}\frac{\sin(k_l r+\theta)}{k_l r}, \tag{6}$$

between turning points [18]. The phase θ will not be important in the following. The WKB wave number $k_l(r)$ is given by

$$k_l^2(r)=\frac{2n_F+3}{a_{osc}^2}-\frac{r^2}{a_{osc}^4}-\frac{l(l+1)}{r^2}. \tag{7}$$

The single-particle energies are

$$\begin{aligned}\epsilon_{n_F,l}-\left(n_F+\frac{3}{2}\right)\hbar\omega&=\int U(r)\mathcal{R}_{n_F l}(r)|^2 r^2 dr\\&=\frac{2}{3\pi}\frac{a}{a_{osc}}(2n_F+3)^{3/2}\hbar\omega\left[\frac{4}{3\pi}-\frac{1}{4\pi}\frac{l(l+1)}{n_F^2}\right].\end{aligned} \tag{8}$$

The latter result is calculated from the overlap between the mean field as given by Eqs. (3) and (5) and the WKB wave functions as given by Eqs. (6) and (7) [14]. It is exact within WKB for $l\ll n_F$ and it compares well to numerical results for all l. For attractive interactions ($a<0$) the lowest-lying states have small angular momentum, which is *opposite* to nuclei.

An important quantity for pairing is the *supergap* which was introduced in Ref. [14] and will be discussed below,

$$G=\frac{32\sqrt{2n_F+3}}{15\pi^2}\frac{|a|}{a_{osc}}\hbar\omega. \tag{9}$$

In comparison the total shell splitting in a shell n_F is, from Eq. (8),

$$D\equiv|\epsilon_{n_F l=n_F}-\epsilon_{n_F l=0}|\simeq\frac{5(n_F+3/2)}{32}G. \tag{10}$$

The pairing depends crucially on the shell splitting D and the supergap G as will be shown in the following section.

III. PAIRING

Pairing in small systems as nuclei [15], metal clusters [3] and superconducting grains [4] appears in odd-even staggering of binding energies, i.e., systems with even number of particles are more strongly bound than odd ones. In nuclei the pairing is also responsible for superfluid effects in collective motion [19].

Pairing in finite systems is described by the Bogoliubov–de Gennes equations [20] and takes place between time-reversed states. As shown in Ref. [15] these states can be approximated by HO wave functions in dilute HO traps as long as the gap does not exceed the oscillator energy, $\Delta\leqslant\hbar\omega$. The gap equation at zero temperature then reduces to

$$\Delta_{nl}=\frac{g}{2}\sum_{n',l'}^{n'\leqslant 2n_F}\frac{2l'+1}{4\pi}\frac{\Delta_{n'l'}}{E_{n'l'}}\int_0^\infty dr\, r^2\mathcal{R}_{nl}^2(r)\mathcal{R}_{n'l'}^2(r), \tag{11}$$

with quasiparticle energies

$$E_{n'l'}=\sqrt{(\epsilon_{n'l'}-\mu)^2+\Delta_{n'l'}^2}. \tag{12}$$

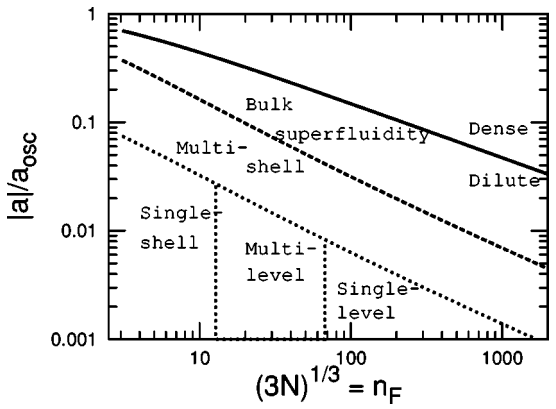

FIG. 1. Diagram displaying the regimes for the various pairing mechanisms (see text) at zero temperature in HO traps vs the number of particles $N=n_F^3/3$ and the interaction strength a. The dotted lines indicate the transitions between single-shell pairing $\Delta=G$, multilevel, Eq. (30), single-level, Eqs. (15)–(17), and multishell pairing, Eq. (24). At the dashed line determined by $2G\ln(\gamma n_F)=\hbar\omega$ the pairing gap is $\Delta\simeq\hbar\omega$, and it marks the transition from multishell pairing to bulk superfluidity, Eq. (25). The pairing gap is $\Delta=0.54E_F$ above the full line $\rho|a|^3\geqslant 1$, which separates the dilute from the dense gas.

The cutoff $n\lesssim 2n_F$ in the sum of the gap equation models as a first approximation the more rigorous regularization procedure described in Ref. [21] that is required for a δ-function pseudopotential.

The chemical potential μ is related to the number of particles by

$$N=2\sum_{n'l'}(2l'+1)\left[1-\frac{\epsilon_{n'l'}-\mu}{E_{n'l'}}\right]. \tag{13}$$

For weak interactions the chemical potential lies within Δ_{nl} from the level energy at the Fermi surface ϵ_{nl}, except for closed levels where the chemical potential lies between the closed and the next open level. For closed shells $N=(n_F+1)(n_F+2)(n_F+3)/3$, the gap vanishes for interactions below a critical value, $G\leqslant G_c=\hbar\omega/2\ln(4\gamma n_F)$ [15].

The gap at the Fermi surface is most important and it is generally proportional to the critical temperature as discussed in the Appendix. For half-filled level (or shell), where $\mu=\epsilon_{n_Fl}$, the gap is equal to the quasiparticle energy $E_{n_Fl}=\Delta_{n_Fl}$. We will in the following refer to this gap as $\Delta\equiv E_{n_Fl}=\Delta_{n_Fl}$.

The HO traps provide a physical system in which the connection between these methods of pairing calculations can be demonstrated and analytical results can be given in various limits of interaction strength and particle number. The associated pairing regimes are displayed in Fig. 1 and will be discussed in the following sections. The first three have been discussed in earlier publications [14,15] but contain additional details of derivations and set the notation. In the remaining three sections, which describe pairing regimes, pairing gaps are calculated and the transitions to the other regimes are discussed. The last section treats the important regime of multilevel pairing which will be shown to be especially relevant for nuclei in the following section.

A. Single-level pairing

For very weak interactions pairing takes place only between time-reversed states $\psi_{lm}(\mathbf{r}_1)\psi_{l-m}(\mathbf{r}_2)$ within the l level at the Fermi surface, i.e., $l'=l$. Maximal pairing between two particles in the level is achieved with the Cooper pair wave function

$$\phi_0(n_F,l)=\sum_m\langle lml-m|00\rangle\psi_{lm}(\mathbf{r}_1)\psi_{l-m}(\mathbf{r}_2). \tag{14}$$

The pairing energy between only two particles in the level is twice the quasiparticle energy, and so

$$E_{n_Fl}=\frac{g}{2}\langle\phi_0(n_F,l)|\delta^3(\mathbf{r}_1-\mathbf{r}_2)|\phi_0(n_F,l)\rangle$$
$$=\frac{g}{2}\frac{2l+1}{4\pi}\int_0^\infty dr\,r^2\mathcal{R}^4_{n_Fl}(r). \tag{15}$$

It follows from the seniority scheme (see, e.g., Ref. [22]) that this is generally the quasiparticle energy and excitation energy for any even number of particles in the level. Solving the gap, Eq. (11), also gives $E_{n_Fl}=\Delta$ for any number of particles in the level.

The pairing energies were given in Ref. [14]. For the top levels $l\simeq n_F$ the HO wave functions are sufficiently simple that the pairing energy can be calculated exactly. For example, $\mathcal{R}^2_{n_Fl=n_F}=[2/\Gamma(l+3/2)]r^{2l}\exp(-r^2)$ (in units where $a_{osc}=1$) which when inserted in Eq. (15) gives the gap

$$E_{n_Fl=n_F}=\frac{|a|}{\sqrt{\pi}a_{osc}}\hbar\omega. \tag{16}$$

The HO wave function for $l=0$ can be approximated by the WKB one of Eq. (6) when $n_F\gg 1$. Inserting in Eq. (15) gives the pair gap [18]

$$E_{n_Fl=0}=\frac{\sqrt{2}}{\pi\sqrt{n_F}}\frac{|a|}{a_{osc}}\hbar\omega. \tag{17}$$

Around midshell, i.e., away from closed ($1\ll l$) and open ($1\ll n_F-l$) shells, the WKB wave functions must be replaced near their turning points by Airy functions, which removes a logarithmic singularity and in turn leads to a logarithm $\ln(l)$. We find [23]

$$E_{n_Fl}=\frac{\sqrt{2}}{\pi^2\sqrt{n_F}}\ln(l)\frac{|a|}{a_{osc}}\hbar\omega,\quad 1\ll l\ll n_F, \tag{18}$$

to leading logarithmic accuracy.

As shown in Fig. 1 the single-level pairing regime appears for sufficiently weak interactions and large number of particles ($n_F\gtrsim 50$) such that $D\gg G$. The corresponding pairing gaps can be seen in Fig. 2 at large n_F.

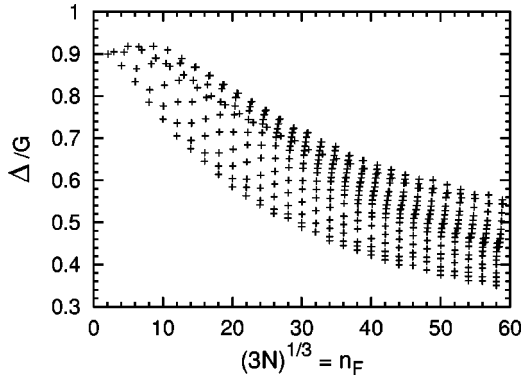

FIG. 2. The pairing gap Δ in units of G vs the number of particles (or n_F) in a trap with half-filled levels calculated from the gap equation (11). The scattering length is $a=-0.01a_{osc}$. The pairing gaps $\Delta_{n_F l}$ are plotted with + for each half-filled level l (only even l and n_F are shown). The gap undergoes a transition from single-shell to multilevel and finally single-level pairing.

B. Single-shell pairing

When n_F is sufficiently small the mean-field splitting D is smaller than the pairing gaps and the pairing acts between all states in an oscillator shell and not just in a single l multiplet, i.e., the full SU(3) symmetry is effectively restored as compared to the SU(2) symmetry of the single l multiplet. This enhanced pairing is referred to as ''SU(3) pairing'' or ''superpairing.'' [14] We shall calculate the gap by writing down the superpair wave function. As in single-level pairing, however, we obtain the same result by solving the gap equation.

Assuming SU(3) symmetry the pairing can be calculated variationally with a pair wave function that is a generalization of Eq. (14) to a sum over $l=n_F,n_F-2,\ldots,1$ or 0,

$$\Phi_0(n_F)=\frac{\sum_l \alpha_l \phi_0(n_F,l)}{\left[\sum_l \alpha_l^2\right]^{1/2}}. \tag{19}$$

The weights α_l can be found by a variational method with the overlap integrals $\int \mathcal{R}_{nl}^2 \mathcal{R}_{n'l'}^2 r^2 dr$ calculated numerically [23]. For large n_F we find $\alpha_l \sim \sqrt{2l+1}$ very accurately. The sums then reduce to the HO level density

$$\sum_{lm} |\psi_{lm}(\mathbf{r})|^2=\frac{1}{4\pi}\sum_l (2l+1)\mathcal{R}_{nl}^2=\frac{\partial \rho_\sigma(r)}{\partial n}.$$

Here, $\rho_\sigma=\rho/2$ is the density of one spin state [see Eq. (5) for $n=n_F$] when shells up to energy $(n+3/2)\hbar\omega$ are occupied and $\partial\rho(r)/\partial n$ is then the density of the nth shell.

The sum over l states in the gap equation simplifies enormously by using the Thomas-Fermi identity valid for $n\gg 1$,

$$\sum_l \frac{(2l+1)}{4\pi}\mathcal{R}_{nl}^2(r)=\frac{\partial\rho_\sigma(r)}{\partial n}=\frac{\sqrt{2n+3}}{2\pi^2 a_{osc}^3}\sqrt{1-\frac{r^2}{R_{TF}^2}}. \tag{20}$$

The pairing energy is thus

$$E_{n_F l}=\frac{g}{2}\langle\Phi_0(n_F)|\delta^3(\mathbf{r}_1-\mathbf{r}_2)|\Phi_0(n_F)\rangle$$

$$=\frac{g}{2}\frac{\int dr\, r^2[\partial\rho_\sigma(r)/\partial n|_{n_F}]^2}{\int dr\, r^2 \partial\rho_\sigma(r)/\partial n|_{n_F}}=G, \tag{21}$$

where the supergap G was given in Eq. (9). The condition for single-shell pairing in atomic HO traps is $D\lesssim 2\Delta=2G$, and is thus $n_F\lesssim 64/5$ according to Eqs. (9) and (10) or, equivalently, to $N\lesssim 10^3$ trapped particles.

For more than two particles in the shell we may again invoke the seniority scheme. It applies approximately to many superpairs when the singlelevel gap is replaced by the supergap G, and the level degeneracy for a full HO shell $\Omega=(n_F+1)(n_F+2)$. Numerical calculations for half-filled shells confirm that the pairing energy per particle is given by the supergap for single-shell pairing [15].

The single-shell pair energy spectrum does, however, differ from that for single-level pairing. In the latter case, one can generally write the pairing wave function in Eq. (14) as any linear combination of the time-reversed two-particle states $\psi_{lm}(\mathbf{r}_1)\psi_{l-m}(\mathbf{r}_2)$. Due to rotational SO(3) symmetry the overlap integrals in a single level are independent of m and the spectrum of pairing energies is particularly simple: one state with $2E_{n_F l}$ as given by Eqs. (16)–(18) and rest of the $(2l+1)$ states has zero energy per pair. In the shell, however, the overlap between the radial wave functions depends on l and l'; the corresponding matrix for $l,l'=n_F,n_F-2,\ldots,1$ or 0 has a nontrivial eigenvalue spectrum: $E_S\simeq 2G/(2S+1)$, $S=0,1,\ldots,\mathrm{Int}[(n_F+1)/2]$, when $n_F\gg 1$ (Int denotes ''integer value'') [23]. The corresponding eigenvectors α_l are very well approximated by Chebyshev's polynomia as function of $x=(l/n_F)^2$ in the large n_F limit. Consequently, the excitation energy of a pair is only 2/3 of the energy $2G$ that it takes to break the pair completely. The richer spectrum is important for expressing an effective Hamiltonian for BCS pairing.

C. Multishell pairing

For increasing interaction strength pairing also takes place between different shells, i.e., $n\neq n_F$ contributes in the sum over n in the gap equation (11). The pairing strength Δ_n depends only weakly on n for the shells around $n=n_F$, which mainly contribute to the pairing and we therefore approximate $\Delta_n\simeq\Delta_{n_F}$. For half-filled shell $\mu=\epsilon_{n_F l}$ and $\Delta_{n_F l}=E_{N_F l}=\Delta$. The gap equation then becomes [15]

$$\Delta=G+G\sum_{n\neq n_F}^{n\lesssim 2n_F}\frac{\Delta}{\sqrt{[(n-n_F)\hbar\omega]^2+\Delta^2}}. \tag{22}$$

The sum can be converted into an integral when correcting the lower limit $n=1$ by $\gamma=e^C$ where $C=0.577\ldots$ is Euler's constant. It then gives to leading orders

$$\Delta \simeq G + 2G\frac{\Delta}{\hbar\omega}\ln\left(\frac{2\gamma n_F}{1+\sqrt{1+(\gamma\Delta/\hbar\omega)^2}}\right), \tag{23}$$

which for $\Delta \ll \hbar\omega$ gives

$$\Delta = \frac{G}{1-2\ln(\gamma n_F)\dfrac{G}{\hbar\omega}}. \tag{24}$$

This is the *multishell pairing* gap valid for interactions such that $G\ln(n_F)/\hbar\omega \lesssim 1/2$. The region of multishell pairing $0.1 \lesssim G\ln(n_F)/\hbar\omega \lesssim 1/2$ extends the single-shell pairing gap G up to stronger interactions where $\Delta \sim \hbar\omega$ (see Fig. 1). Cooper pairs are still essentially only formed between states within the same shell. However, there is pairing in many shells besides that at the Fermi level resulting in a gap that is larger than $\Delta = G$.

D. Bulk superfluidity

For a large system the local superfluid field is related to that in a uniform system. In the TF approximation the local pairing field then depends on radius,

$$\Delta(r) = \kappa\frac{k_F^2(r)}{2m}\exp\left(\frac{\pi}{2ak_F(r)}\right), \tag{25}$$

where $k_F(r) = [3\pi^2\rho(r)]^{1/3} = \sqrt{2n_F - r^2/a_{osc}^2}/a_{osc}$ is the TF wave number. The prefactor is $\kappa = 8/e^2$ without and $\kappa = (2/e)^{7/3}$ with corrections from induced interactions [24].

When the attractions are sufficiently strong and/or the number of particles in the trap large enough such that $G\ln(\gamma n_F) \gtrsim \hbar\omega$, the pairing field exceeds the HO frequency in the bulk of the trap except in a narrow surface region. For that reason the low-lying single-particle excitations [25,15] and the collective modes are surface modes with typical excitation energies of the order of $\sim\hbar\omega$ [26]. For example, the lowest s-wave excitation (the monopole) is $\omega_0 = 2\omega$ in the collisionless limit. This is in contrast to the weakly interacting system, i.e., below the bulk superfluidity region of Fig. 1, where $\omega_0 = \Delta$ for open shells. We refer to Refs. [15,26] for a discussion of such modes.

Here, we concentrate on the bulk superfluid field inside the trap and will relate it to that in a uniform system. Contrary to the surface states, the excitations at higher energies are less affected by the pairing field and the Bogoliubov wave functions are approximately given by the unperturbed HO wave functions. Consequently, the intrashell pairing condition discussed in Ref. [15], which leads to the gap equations (11) and (22), is approximately valid for these states. However, the gap is to be understood as an average superfluid gap $\langle\Delta\rangle$ in bulk. The gap equation (23) is readily solved when $\langle\Delta\rangle \gtrsim \hbar\omega$,

$$\langle\Delta\rangle \simeq 2n_F\hbar\omega\exp(-\hbar\omega/2G). \tag{26}$$

We now observe that the exponent in Eq. (26) coincides with that in the TF-BCS Eq. (25) when the Fermi wave number is replaced by its spatial average in a finite system:

$$\langle k_F(r)\rangle \equiv \frac{\int k_F^2(r)d^3r}{\int k_F(r)d^3r} = \frac{32}{15\pi}k_F(0), \tag{27}$$

where $k_F(0) = \sqrt{2n_F}/a_{osc}$. That the spatial average should be performed over $k_F(r)^2$ follows from Eq. (9) where the factor $\partial\rho(r)/\partial n \propto k_F(r)$ of Eq. (20) enters twice. By definition of the supergap we find that $\hbar\omega/G = \pi/2|a|\langle k_F(r)\rangle$, and the two exponents match. The prefactors differ due to the approximate cutoff $n \lesssim 2n_F$ in the gap equation, the approximate treatment of the overlap integrals and their n dependence in the gap equation leading to Eq. (26).

E. Dense liquid

The *dense* or strongly interacting limit $k_F|a| \gtrsim 1$ can be encountered near a Feshbach resonance where $a \to -\infty$. In this regime the dilute gas approximation implicit in the interactions in the Hamiltonian (1) is no longer valid and a new scaling region appears [6–8,12,13]. Both the energy per particle and the pairing gap approach a finite fraction of the Fermi energy. Recent Green's-function Monte Carlo calculations [13] find that the interaction energy is -0.56 times the kinetic energy and that the odd-even staggering energy or pairing gap in bulk is $\Delta \simeq 0.54E_F$.

F. Multilevel pairing

We finally address the intermediate regime $G \gtrsim D \gtrsim \Delta$ (see Fig. 1) which lies between the single-level, single-shell, and multishell pairing regions studied above. Here, pairing takes place between multiple (l,l') levels lying close to the Fermi surface $\mu \simeq \varepsilon_{n_F,l}$, and will therefore be referred to as *multilevel pairing*. This region overlaps the regions studied in the above sections and therefore applies to most systems of trapped fermions except traps with very few (single-shell), very many (single-level), or strongly interacting fermions (multishell). As we shall see below nuclei can also be considered to belong to the multilevel regime.

For large level splitting $D \gg \Delta$ the detailed structure of the overlap integrals in Eq. (11) becomes important. We shall calculate these analytically using WKB as well as numerically from the exact HO radial wave functions. Inserting the latter in the gap equation we calculate the pairing gaps as shown in Figs. 2 and 3 for half-filled levels, i.e., for $\mu = \varepsilon_{n_F l}$, where $E_{n_F l} = \Delta_{n_F l} = \Delta$.

A qualitative understanding of these results can be obtained from analytical WKB calculations. At large n_F the WKB wave functions $\mathcal{R}_{n_F l}$ of Eq. (6) are excellent approximations except for the multilevel overlap $l = l'$ where a logarithmic singularity appears, which was responsible for the $\ln(l)$ in Eq. (18). Otherwise, when $0 < |l^2 - l'^2| \ll n_F^2$ the overlap integral of the WKB wave functions of Eq. (6) is dominated by the overlap near the turning points. Defining $\xi = 2n_F(r/a_{osc})^2 - (r/a_{osc})^4$, the overlap is

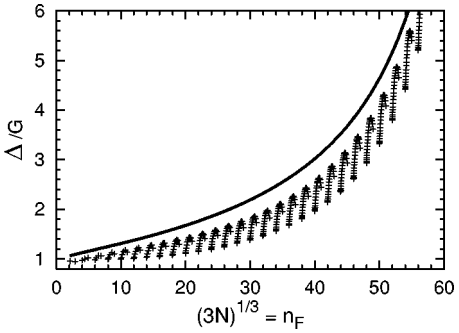

FIG. 3. Same as Fig. 2 but with $a=-0.04a_{osc}$. Full line is the multishell gap $G/[1-2\ln(\gamma n_F)G/\hbar\omega]$. The gap undergoes a transition from single shell to a mixture of multilevel and multishell pairing.

$$\int_0^\infty dr\, r^2 \mathcal{R}^2_{n_F l}(r)\mathcal{R}^2_{n_F l'}(r) \propto \left(\frac{4}{\pi}\right)^2 \int \frac{dr}{\sqrt{\xi-l^2}\sqrt{\xi-l'^2}} \propto -\ln(|x-x'|), \tag{28}$$

to leading logarithmic order, where $x=(l/n_F)^2$ and $x'=(l'/n_F)^2$. This logarithmic dependence of the matrix element has the interesting consequence that it leads to a *double log* in the gap equation. When the energy factor $1/E_{nl'} \simeq [D^2(x-x')^2+\Delta^2]^{-1/2}$ is summed over l' or, equivalently when $n_F \gg 1$, integrated over x', it leads to the (usual) factor $\ln(D/\Delta)$. The other logarithm appears from the matrix element of Eq. (28) which, when summed over l' in the gap equation with the energy factor, attains the lower cutoff at $|x-x'| \simeq \Delta/D$. It is assumed that the l dependence of the gap is sufficiently weak within the levels over which pairing takes place, i.e., $\Delta \ll D$, which is supported by numerical results (see Figs. 2 and 3). The gap equation then reduces to

$$1 \simeq \alpha(x) G \int_0^1 dx' \frac{-\ln|x-x'|}{\sqrt{D^2|x-x'|^2+\Delta^2}} \simeq \alpha(x)\frac{G}{D}\ln^2[\beta(x)D/\Delta] \tag{29}$$

to leading logarithmic orders. The factors $\beta(x)$ and $\alpha(x)$ both depend on $x=(l/n_F)^2$, but not on l or n_F separately. Only G and D depend on n_F explicitly.

The resulting multilevel gap is

$$\Delta = \beta(x) D \exp[-\sqrt{D/G\alpha(x)}]. \tag{30}$$

At midshell $x=1/2$, the exponent can be calculated as $\alpha(1/2) \simeq 15/32\sqrt{2}$ and the prefactor $\beta(1/2)=2e$ to leading logarithmic order for large n_F. Near open ($l=0$) and closed ($l=n_F$) shells there are generally only half as many states to pair with which reduces $\alpha(x=0)$ and $\alpha(x=1)$ by a factor $\sim 1/2$ on average. However, as the matrix elements are larger for $l \simeq n_F$ but smaller for $l=0$ [see Eq. (28)], the gaps become asymmetric with a maximum above midshell. Such a shell structure is also found in the multilevel pairing regime when the gap equation is solved numerically with the exact HO wave functions as is shown in Figs. 2 and 3.

Two illustrative examples are shown in Figs. 2 and 3. In the first the coupling is sufficiently weak, $a=-0.01a_{osc}$, that the pairing undergoes transitions from single shell at small n_F to multilevel for $10 \lesssim n_F \lesssim 40$ and finally single-level pairing for large n_F. In Fig. 3 the coupling is stronger, $a=-0.04a_{osc}$, and the pairing undergoes transitions from single shell to multilevel and approaches multishell pairing for large n_F. These transitions between pairing regimes are illustrated in Fig. 1.

The multilevel gap of Eq. (30) is quite robust and applies to many systems as long as $G \gtrsim D \gtrsim \Delta$. Its validity for nuclei will be discussed below. The formula for the multilevel gap can be generalized by relating the shell splitting to the density of states at the Fermi surface as $\partial n/\partial\epsilon = \Omega/D$, where $\Omega = n_F^2$ is the number of states in the shell. Likewise, the supergap is related to the coupling constant as $G \propto g\Omega$. If the level spectrum of Eq. (8) is changed, the multilevel gap remains valid, if the shell splitting is correspondingly scaled with the level density. In other words the double log does not depend on the details of the level spectrum but is generic for systems such as HO traps, because the one log is associated with the overlap matrix elements between nearby states and the other is associated with the quasiparticle energy in the gap equation.

The appearance of a double log is not unique for multilevel pairing but also occurs in the case of color superconductivity in quark matter [27]. The physical mechanism behind this is, however, different. Within perturbative QCD the singular quark-quark interaction g_{QCD}/q^2, where q is the momentum transfer carried by a gluon, is dynamically screened by Landau damping. When the interaction is integrated over momentum and energy transfer, the dynamical screening leads to a logarithm of the gap. Thus it is the interactions that are responsible for the second logarithm and not the wave function overlap of nearby states as in the HO trap.

IV. PAIRING IN NUCLEI

The nuclear mean field is often approximated by a simple HO form and the residual effective pairing interaction by a δ force in order to obtain some qualitative insight into single-particle levels, pairing, collective motion, etc. (see, e.g., Refs. [19,22]). We can therefore compare pairing in nuclei to that in traps as investigated above, once the HO potential is adjusted to describe nuclei. We emphasize that we do not intend to calculate the quantitative pairing gaps for each individual nucleus which would require detailed knowledge of the individual level spectra, deformation, many-body effects, etc. Instead we aim at qualitative results for the pairing gap dependence on mass number, shell effects, and to extrapolate to very large nuclei, nuclear, and neutron star matter.

Large nuclei have approximately constant central density $\rho_0 \simeq 0.14$ fm^{-3} and Fermi energy E_F in bulk. Therefore the HO frequency, which is fitted to the nuclear mean field, decreases with the number of nucleons $A=N+Z$, where N

now is the number of neutrons and Z the number of protons in the nucleus, as

$$\hbar\omega \simeq E_F/n_F \simeq 41\ \mathrm{MeV}\times A^{-1/3}. \tag{31}$$

In the valley of β stability the number of protons is $Z \simeq A/(2+0.0155A^{2/3})$.

Second, the nuclear mean field deviates from a HO potential by being almost constant inside the nucleus and vanishes outside. The resulting net anharmonic nuclear field is *stronger* and *opposite* in sign to the corresponding (anharmonic) mean field in atomic traps. Therefore, the level splitting is larger and the ordering of the l levels is reversed. In addition, a strong spin-orbit force splits the single-particle states of total angular momentum $j=l\pm 1/2$, such that the $j=n_F+1/2$ is lowered down to the shell (n_F-1) below.

Proton and neutron pairing gaps are typical of the order of ~ 1 MeV in nuclei, i.e., smaller than both $\hbar\omega$ and D but of the order of the average splitting between two adjacent j levels. Consequently, nuclei can be considered as HO traps with a level splitting D such that they fall into the multilevel pairing regime. However, the number of particles in nuclei is relatively small so that nuclei are close to the single-shell pairing regime. Furthermore, the interactions are so strong that multishell pairing also becomes important. From the results of Sec. III we can predict several features of neutron and proton pairing gaps.

(1) Mass scaling: Since $\hbar\omega$ scale as $\sim A^{-1/3}$ and $a_{osc} \propto n_F^{1/2}$ [see Eq. (9)] the single-shell pairing gap also scales as $G\sim A^{-1/3}$. The level splitting tends to reduce the pairing towards the multilevel gap but is compensated by multishell pairing. Therefore, the pairing gaps in light and medium mass nuclei scale approximately as $\Delta \simeq G \propto A^{-1/3}$.

(2) Shell structure: The pairing gaps should exhibit a strong shell structure similar to those for multilevel pairing (Figs. 2 and 3), however with reversed l since D is negative for nuclei. Due to the strong spin-orbit force the $j=l\pm 1/2$ states are split and the $j=n_F+1/2$ is lowered down to the shell below. The magic numbers become $N,Z=8,14,28,50,82,126,184,\ldots$, etc. rather than the HO filled shell particle numbers $N,Z=2,8,20,40,70,112,168,240,\ldots$, etc.

(3) Bulk limit for large nuclei/nuclear matter: For very large nuclei multishell pairing becomes important and pairing approaches that in bulk matter. By fitting the effective nucleon coupling constant to pairing gaps in finite nuclei we will below estimate the pairing in nuclear matter from Eq. (25).

These predictions agree qualitatively with experimental data (see Figs. 4 and 5).

For a more quantitative calculation the level spectrum must be specified. Instead of fitting the level spectrum for each nucleus with a correspondingly large number of adjustable parameters, we make the following simplifying approximation analogous to the single-particle spectrum of Eq. (8):

$$\epsilon_{nj} = \left(n+\frac{3}{2}\right)\hbar\omega - D\frac{j(j+1)}{(n+1/2)(n+3/2)}. \tag{32}$$

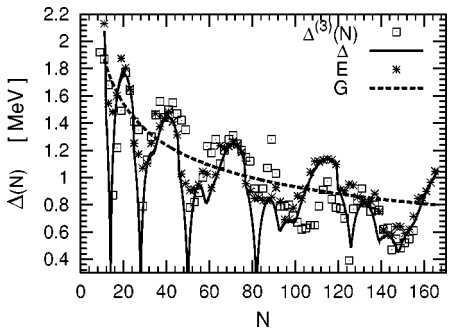

FIG. 4. Neutron pairing energies vs the number of neutrons. The experimental odd-even staggering energies $\Delta^{(3)}(N)$ are averaged over isotopes [28,29]. The calculated gaps Δ and quasiparticle energies E are obtained from the gap equation (see text) with effective coupling strength $a=-0.41$ fm. The supergap G is shown with dashed line.

The level splitting is approximated by $D=0.13(n_F+3/2)\hbar\omega$ in analogy with Eq. (10) and based on nuclear structure calculations, which generally find that the level splitting increases with shell number and is of the order of $D\simeq\hbar\omega$ for heavy nuclei $(n_F\sim 6)$. The spin-orbit splitting and resulting change in magic numbers are incorporated to first approximation by simply moving the lowest level in each shell down to the shell below, i.e., $D=\hbar\omega$ for $j=n_F+1/2$.

The pairing gaps and quasiparticle energies can now be calculated by solving the gap equation inserting the HO matrix elements and with $\hbar\omega$ and level splitting as given by Eqs. (31) and (32). The effective strength a is then the only adjustable parameter.

The data on neutron and proton pairing are obtained from the odd-even staggering of nuclear binding energies $B(N,Z)$. It has been shown that mean-field contributions can be removed [29] by using the three-point filter

$$\Delta^{(3)}(N) \equiv \frac{(-1)^N}{2}[B(N-1,Z)+B(N+1,Z)-2B(N,Z)], \tag{33}$$

when N is an odd number of neutrons. The analogous relation is valid for protons.

The total binding energies are elaborate sums over quasiparticle energies weighted with occupation numbers. Mean-field energies and single-particle energies should also be in-

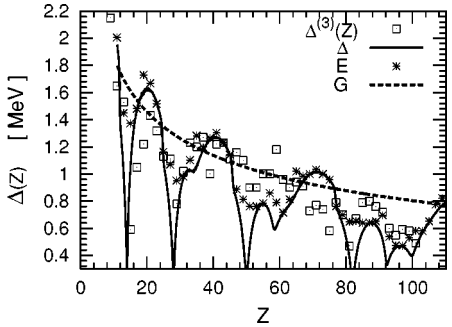

FIG. 5. Same as Fig. 4 but for protons.

cluded self-consistently. Furthermore, the Bogoliubov transformation does not preserve exact particle number and does not treat a single unpaired particle that appears in odd-number systems. Also nuclear spectra are complicated by deformations and the finite range, spin and spin-orbit dependences of the nucleon-nucleon interaction [19,30]. For these reasons we cannot calculate $\Delta^{(3)}$ directly. Instead we will for simplicity compare to the quasiparticle energies and pairing gaps, which are calculated directly from the gap equation as function of $\mu(N,Z)$. It has been argued (see, e.g., Ref. [29] and references herein) that mean-field effects cancel in the quasiparticle energy for odd particle number and that it therefore may be compared to the corresponding three-point energies. However, as particle number fluctuations, deformations, possible mean-field energy corrections, and other effects are not included, the pairing gaps are also shown in Figs. 4 and 5 for comparison. They are equal to the quasiparticle energy for half-filled levels only and generally smaller especially at the magic numbers where the gaps vanish in several cases.

We compare in Fig. 4 the experimental $\Delta^{(3)}(N)$ averaged over isotopes with the calculated gaps $\Delta_{n_F l}$, and in Fig. 5 the analogous for protons $\Delta^{(3)}(Z)$ averaged over isotones. In the calculations the effective coupling is the only parameter fitted to experimental data. For both neutrons and protons we extract $a \simeq -0.41$ fm.

We note that although the neutron pairing gaps in Fig. 4 are generally larger than the proton ones in Fig. 5, this is not reflected in the effective coupling constants. The reason is the asymmetry of heavy nuclei. For example, for $N=82$ the mass number is $A \simeq 140$ whereas for $Z=82$ it is $A \simeq 208$. The mass numbers enter both D and G and lead to a reduction of the proton pairing gap relative to the neutron one by just the right amount so that the experimental data on neutron and proton odd-even staggering can be fitted with the same pairing strength $a=-0.41$ fm.

Considering the simplicity of the model it describes a large number of experimental gaps fairly well on average. In a number of cases, however, the calculated pairing gaps differ significantly from the measured neutron gaps. Some of these deviations can be attributed to the crude single-particle level spectra assumed. If the single-particle level energies are adjusted according to more detailed mean-field calculations (see, e.g., Ref. [19]) the agreement with experimental pairing gaps improves in several cases.

The pairing gaps are sensitive to the shell splitting and the coupling. The uncertainty in the coupling is smaller because the changes in D affects both the exponent and the prefactor in the gap of Eq. (30) in a compensating way. Another uncertainty arises from the upper cutoff. Whereas HO traps can pair between shells up to $\sim 2n_F$, nuclei have a continuum of states at about the binding energy per nucleon $E_B \simeq 8$ MeV above the Fermi level. Therefore the sum over shells in the gap equation has been limited to $n \lesssim (E_F+E_B)/\hbar\omega$, which for medium mass nuclei corresponds to $n \lesssim n_F+1$, with a smooth cutoff as in Ref. [31]. The pairing gaps are, however, only logarithmically sensitive to this cutoff.

Nuclei can also be deformed around midshell, which increases pairing [29]. These and other nuclear many-body effects must be included in a more quantitative study of pairing in individual nuclei. For this purpose it will be useful also to study pairing in elongated atomic traps with deformations as in nuclei. Near closed shells pairing reduces or inhibits deformations. The effect of pairing is also observed in rotational spectra where the moment of inertia is reduced from the rigid to superfluid or irrotational value [19]. In traps the external HO potential generally dominates over the mean-field interaction energy and thus does not deform spontaneously [32] as in nuclei—unless of course if the HO trap itself is deformed.

Nuclei cannot directly be placed in any of the various pairing phases of Fig. 1 because the level splitting is larger than for trapped atoms. The effective scattering length $a=-0.41$ fm and $a_{osc} \simeq 1$ fm$/\sqrt{n_F}$ would place nuclei with masses up to $A=250$ corresponding to $n_F \lesssim 6$ in the upper left corner of Fig. 1 in the multishell region. However, because D is much larger in nuclei than for trapped atoms, the multilevel pairing region extends down to lower n_F and up to larger strengths $|a|$. Furthermore, the continuum of states in nuclei reduces the effect of multishell pairing as discussed above. Therefore, nuclei rather belong to the transition region between single-shell, multishell, and multilevel pairing.

The best fit to odd-even staggering energies of nuclei determines $a=-0.41$ fm accurately. Systematic errors may, however, be expected from the approximations implicit in the level splitting, the cutoff, and in approximating $\Delta^{(3)}$ by Δ. However, because the multilevel and the multishell pairing partly compensate, a good approximation to the average gap in nuclei is the single-shell supergap

$$\Delta \simeq G \simeq \frac{|a|}{0.41\ \text{fm}} \frac{5.5\ \text{MeV}}{A^{1/3}}. \tag{34}$$

This supergap is also shown in Figs. 4 and 5. It does not depend on the level splitting or cutoff and is therefore a robust prediction for the average magnitude and mass scaling of pairing gaps in nuclei.

Empirically the pairing term in Bethe-Weiszäcker liquid-drop formula, $\Delta \simeq 12\ \text{MeV} \times A^{-1/2}$, fits the odd-even staggering energies of nuclei with $A \lesssim 250$ averaged over shell effects. The scaling with mass number can now be understood in terms of the supergap with shell corrections. If D was a constant times $\hbar\omega$ then the multilevel gap of Eq. (30) would also scale as $A^{-1/3}$. However, because D increases with $n_F \propto A^{-1/3}$, the multilevel gap decreases faster with A for small and medium mass nuclei but slower for heavy nuclei due to multishell pairing. Both are in accordance with the empirical mass dependence.

The pairing in nuclear matter can also be estimated once the effective interaction has been determined. Inserting in Eq. (25) $a=-0.41$ fm and $k_F=1.33\ \text{fm}^{-1}$ at nuclear saturation density, $\rho_0=0.15\ \text{fm}^{-1}$, we obtain the proton and neutron pairing gaps,

$$\Delta \simeq 1.1\ \text{MeV}, \tag{35}$$

in the bulk of very large nuclei and in symmetric nuclear matter at nuclear saturation density. This number is compatible with earlier calculations [33] of the $^1S_0$ pairing gap in nuclear and neutron star matter around normal nuclear matter densities. A smaller value for bulk pairing might have been expected from Figs. 4 and 5 by extrapolating the odd-even staggering energies of heavy nuclei to higher mass numbers. However, as $A \propto n_F^3$ becomes large the multishell pairing contributes with the increasing term $\ln(n_F)$ in the gap equation. Therefore the bulk value is larger than the pairing gap in heavy nuclei which also have a smaller cutoff due to continuum states as discussed above.

Neutron star matter has a wide range of densities and is very asymmetric, $Z/A \simeq 0.1$. One can attempt to estimate the pairing gaps as function of density from the gap in bulk, Eq. (11), with $a \simeq -0.41$ fm and the neutron or proton Fermi wave numbers $k_F^{N,Z} = (3\pi^2 \rho_{N,Z})^{1/3}$ as function of densities. However, the effective interaction a is density dependent. At higher densities we expect the effective interaction to become repulsive as is the case for the nuclear mean field at a few times nuclear saturation density. At lower densities the effective scattering length should approach that in vacuum which for neutron-neutron scattering is $a(^1S_0) \simeq -18$ fm. This dilute limit $k_F|a| \ll 1$ does, however, require extremely low densities as compared to normal nuclear matter density.

V. SUMMARY

Pairing gaps have been calculated for ultracold atomic Fermi gases in harmonic-oscillator traps and compared to nuclei. The pairing mechanism was found to be similar for these systems in the sense that the spacing between single-particle states (and shells) reduces the pairing over several of these levels near the Fermi surface referred to as multilevel pairing. At low particle densities the shell structures in traps are pronounced as they are in nuclei and the level degeneracies are important for the size of the gaps which can differ substantially from those known from homogeneous systems [24] and systems with continuous level densities.

Neutron and proton pairing gaps in nuclei were calculated and with an effective coupling strength $a = -0.41$ fm a qualitative description of their shell structure could be given, and the average pairing gaps were found to scale with mass number approximately as $\Delta \simeq 5.5\ \mathrm{MeV}/A^{1/3}$ as predicted from the supergap. Eventually for large mass number the gap approaches the $^1S_0$ superfluid gap in uniform nuclear matter, which was calculated as $\Delta \simeq 1.1$ MeV for both neutrons and protons.

Mixing fermionic with bosonic atoms improves cooling [34,9] to lower temperatures so that weak pairing can also be studied, and the additional induced interactions between fermions and bosons generally enhance pairing [24]. Furthermore, the shell splitting can be changed in a controlled way by the number of bosons in the trap and the sign and strength of their interaction with the fermions.

The similarity of multilevel and bulk pairing in atomic traps and nuclei may provide new insight into pairing and superfluidity in nuclei and neutron star matter from tabletop experiments at low temperatures.

APPENDIX: CRITICAL TEMPERATURES

The pairing gaps generally decrease with increasing temperature from its zero-temperature value $\Delta(T=0)$, which was calculated above, to the critical temperature T_c, where it vanishes. The temperature dependence of the gap and T_c itself are determined from

$$\Delta_{n_F,l}(T) = \sum_{n'l'} [1 - 2f(E_{n',l'}/T)] \frac{\Delta_{n',l'}(T)}{E_{n',l'}} \frac{g}{4\pi} \times \int_0^\infty dr\, r^2 \mathcal{R}^2_{nl}(r) \mathcal{R}^2_{n'l'}(r), \tag{A1}$$

with $E_{n'l'} = \sqrt{(\epsilon_{n'l'} - \mu)^2 + \Delta^2(T)}$.

As shown in Ref. [35] T_c is exactly half of the zero-temperature gap

$$T_c = G/2[1 - 2\ln(\gamma n_F) G/\hbar\omega] = \tfrac{1}{2}\Delta(T=0), \tag{A2}$$

in the single-shell and multishell pairing regimes, and this also applies to the single-level pairing regime.

In uniform Fermi gases the critical temperature is [24]

$$T_c = \frac{\gamma}{\pi} \kappa E_F \exp(2/\pi a k_F) = \frac{\gamma}{\pi}\Delta(T=0). \tag{A3}$$

The ratio $T_c/\Delta(T=0) = \gamma/\pi \simeq 0.567$ is the same irrespective of whether induced interactions are included or not.

In the multilevel regime T_c can be determined from Eq. (A1) with overlap integrals as given in Eq. (28). To leading logarithmic order we find for large n_F

$$T_c = \frac{\gamma}{\pi}\Delta(T=0). \tag{A4}$$

That $T_c/\Delta(T=0) = \gamma/\pi$ as in the uniform Fermi gas is mainly because the pairing takes place over several l levels and the level density therefore is effectively continuous. The overlap integrals do not change this ratio to leading logarithmic order.

Although $T_c/\Delta(T=0) = \gamma/\pi \simeq 0.567$ is close numerically to the value 1/2 found in the single-shell, single-level, and multishell regimes, the difference reveals the qualitative differences in the underlying level spectrum, namely, continuous vs discrete, respectively.

Near a Feshbach resonance the strongly interacting Fermi gas becomes unstable towards molecule formation. T_c for BCS superfluidity is expected to crossover towards the slightly smaller critical temperature for forming a Bose-Einstein condensate (BEC) of molecules [36]. Both the BCS and BEC critical temperatures are, however, above the lowest temperatures achieved recently for trapped Fermi atoms [5,6,9] if we assume $T_c \simeq 0.5\Delta$ as in Eqs. (A2)–(A4) and take $\Delta = 0.54 E_F$ according to Ref. [13].

[1] J. Bardeen, L.N. Cooper, and J.R. Schrieffer, Phys. Rev. **108**, 1175 (1957).
[2] A. Bohr, B.R. Mottelson, and D. Pines, Phys. Rev. **110**, 936 (1958).
[3] W.A. de Heer, Rev. Mod. Phys. **65**, 611 (1993).
[4] C.T. Black, D.C. Ralph, and M. Tinkham, Phys. Rev. Lett. **76**, 688 (1996).
[5] M.J. Holland, B. DeMarco, and D.S. Jin, Science **285**, 1703 (1999); B. DeMarco, S.B. Papp, and D.S. Jin, Phys. Rev. Lett. **86**, 5409 (2001); A.G. Truscott *et al.*, Science **291**, 2570 (2001); F. Schreck *et al.*, Phys. Rev. A **64**, 011402 (2001); K.M. O'Hara *et al.*, Phys. Rev. Lett. **85**, 2092 (2000).
[6] K.M. O'Hara, S.L. Hemmer, M.E. Gehm, S.R. Granade, and J.E. Thomas, Science **298**, 2179 (2002); M.E. Gehm, S.L. Hemmer, S.R. Granade, K.M. O'Hara, and J.E. Thomas, e-print cond-mat/0212499.
[7] C.A. Regal and D.S. Jin, e-print cond-mat/0302246.
[8] T. Bourdel *et al.*, e-print cond-mat/0303079.
[9] Z. Hadzibabic, S. Gupta, C.A. Stan, C.H. Schunck, M.W. Zwierlein, K. Dieckmann, and W. Ketterle, Phys. Rev. Lett. **91**, 160401 (2003).
[10] H.T.C. Stoof, M. Houbiers, C.A. Sackett, and R.G. Hulet, Phys. Rev. Lett. **76**, 10 (1996).
[11] C. Menotti, P. Pedri, and S. Stringari, Phys. Rev. Lett. **89**, 250402 (2002)
[12] H. Heiselberg, Phys. Rev. A **63**, 043606 (2001).
[13] J. Carlson, S-Y. Chang, V.R. Pandharipande, and K.E. Schmidt, Phys. Rev. Lett. **91**, 050401 (2003).
[14] H. Heiselberg and B.R. Mottelson, Phys. Rev. Lett. **88**, 190401 (2002).
[15] G.M. Bruun and H. Heiselberg, Phys. Rev. A **65**, 053407 (2002).
[16] C.J. Pethick and H. Smith, *Bose-Einstein Condensation in Dilute Gases* (Cambridge University Press, Cambridge, 2002).
[17] For a finite number of particles the factors $n_F+3/2$ include a correction to n_F, which has been checked numerically to improve the TF approximation.
[18] The WKB approximation can be applied between the turning points $r_\pm^2=[n_F+3/2\pm\sqrt{(n_F+3/2)^2-l(l+1)}]a_{osc}^2$. Near the turning points the wave functions must be replaced by Airy functions for detailed gap calculations. The phase θ is only important to leading log order when $l=0$ where $\theta=0$. When the wave function has many nodes $1\ll l\ll n_F$, the oscillations can be averaged as $\langle\sin^2(k_l r)\rangle=1/2$ and $\langle\sin^4(k_l r)\rangle=3/8$.
[19] A. Bohr and B.R. Mottelson, *Nuclear Structure* (Benjamin, New York, 1969), Vols. I and II.
[20] P.G. de Gennes, *Superconductivity of Metals and Alloys* (Addison-Wesley, New York, 1989).
[21] G.M. Bruun, Y. Castin, R. Dum, and K. Burnett, Eur. Phys. J. D **9**, 433 (1999).
[22] A.L. Fetter and J.D. Walecka, *Quantum Theory of Many-Particle Systems* (McGraw-Hill, New York, 1971).
[23] C. Strømfeld, MSc. thesis, Niels Bohr Institute, 2002 (unpublished).
[24] L.P. Gorkov and T.K. Melik-Barkhudarov, JETP Lett. **13**, 1018 (1961); H. Heiselberg, C.J. Pethick, H. Smith, and L. Viverit, Phys. Rev. Lett. **85**, 2418 (2000).
[25] M.A. Baranov, JETP Lett. **70**, 396 (1999); M.A. Baranov and D.S. Petrov, Phys. Rev. A **62**, 041601 (2000).
[26] G.M. Bruun and C.W. Clark, Phys. Rev. Lett. **83**, 5415 (1999); G.M. Bruun and B.R. Mottelson, *ibid.* **87**, 270403 (2001).
[27] D.T. Son, Phys. Rev. D **59**, 094019 (1999).
[28] G. Audi and A.H. Wapstra, Nucl. Phys. **A595**, 409 (1995).
[29] J. Dobaczewski *et al.*, Phys. Rev. C **63**, 024308 (2001).
[30] P. Ring and P. Schuck, *The Nuclear Many-Body Problem* (Springer, Heidelberg, 2000).
[31] M. Bender *et al.*, Eur. Phys. J. A **8**, 59 (2000).
[32] H. Heiselberg and B.R. Mottelson (unpublished).
[33] G. Baym and C.J. Pethick, Annu. Rev. Astron. Astrophys. **17**, 415 (1979); H. Heiselberg and V.R. Pandharipande, Annu. Rev. Nucl. Part. Sci. **50**, 481 (2000); H. Heiselberg and M. Hjorth-Jensen, Phys. Rep. **50**, 481-524 (2000).
[34] H.T.C. Stoof, Phys. Rev. A **61**, 053601 (1999).
[35] G.M. Bruun, Phys. Rev. A **66**, 041602 (2002).
[36] P. Nozières and S. Schmidt-Rink, J. Low Temp. Phys. **59**, 195 (1982); C.A.R. Sá de Melo, M. Randeria, and J.R. Engelbrecht, Phys. Rev. Lett. **71**, 3202 (1993).